



HAL
open science

**MISSENSE MUTATIONS IN THE AFG3L2
PROTEOLYTIC DOMAIN ACCOUNT FOR 1.5% OF
EUROPEAN AUTOSOMAL DOMINANT
CEREBELLAR ATAXIAS**

Claudia Cagnoli, Giovanni Stevanin, Alessandro Brussino, Cecilia Mancini,
Russell Margolis, Susan Holmes, Marcello Nobili, Sylvie Forlani, Sergio
Padovan, Patrizia Pappi, et al.

► **To cite this version:**

Claudia Cagnoli, Giovanni Stevanin, Alessandro Brussino, Cecilia Mancini, Russell Margolis, et al.. MISSENSE MUTATIONS IN THE AFG3L2 PROTEOLYTIC DOMAIN ACCOUNT FOR 1.5% OF EUROPEAN AUTOSOMAL DOMINANT CEREBELLAR ATAXIAS. Human Mutation, 2010, 31 (10), pp.1117. 10.1002/humu.21342 . hal-00574001

HAL Id: hal-00574001

<https://hal.science/hal-00574001>

Submitted on 7 Mar 2011

HAL is a multi-disciplinary open access archive for the deposit and dissemination of scientific research documents, whether they are published or not. The documents may come from teaching and research institutions in France or abroad, or from public or private research centers.

L'archive ouverte pluridisciplinaire **HAL**, est destinée au dépôt et à la diffusion de documents scientifiques de niveau recherche, publiés ou non, émanant des établissements d'enseignement et de recherche français ou étrangers, des laboratoires publics ou privés.



MISSENSE MUTATIONS IN THE AFG3L2 PROTEOLYTIC DOMAIN ACCOUNT FOR ~1.5% OF EUROPEAN AUTOSOMAL DOMINANT CEREBELLAR ATAXIAS

Journal:	<i>Human Mutation</i>
Manuscript ID:	humu-2010-0123.R1
Wiley - Manuscript type:	Rapid Communication
Date Submitted by the Author:	15-Jul-2010
Complete List of Authors:	<p>Cagnoli, Claudia; University of Turin, Genetics Biology and Biochemistry Stevanin, Giovanni; INSERM/UPMC UMR_S975 Brussino, Alessandro; University of Turin, Genetics Biology and Biochemistry Mancini, Cecilia; University of Turin, Genetics Biology and Biochemistry Margolis, Russell; Johns Hopkins University School of Medicine Holmes, Susan; Johns Hopkins University School of Medicine Nobili, Marcello; Division of Neurology, Martini Hospital Forlani, Sylvie; INSERM/UPMC UMR_S975 Padovan, Sergio; cnr Pappi, Patrizia; University of Turin, Genetics Biology and Biochemistry Zaros, Cecile; INSERM/UPMC UMR_S975 Le Ber, Isabelle; INSERM/UPMC UMR_S975 Ribai, Pascale; INSERM/UPMC UMR_S975 Pugliese, Luisa; SAFAN bioinformatics assalto, corrado; SAFAN bioinformatics Brice, Alexis; INSERM U679, Hôpital de la Salpêtrière Migone, Nicola; University of Turin, Genetics Biology and Biochemistry Durr, Alexandra; INSERM U679, Hôpital de la Salpêtrière Brusco, Alfredo; University of Turin, Department of Genetics Biology and Biochemistry</p>
Key Words:	Autosomal Dominant Cerebellar Ataxia, Spinocerebellar ataxia, SCA28, AFG3L2, mutation screening

1
2
3
4
5
6
7
8
9
10
11
12
13
14
15
16
17
18
19
20
21
22
23
24
25
26
27
28
29
30
31
32
33
34
35
36
37
38
39
40
41
42
43
44
45
46
47
48
49
50
51
52
53
54
55
56
57
58
59
60

SCHOLARONE™
Manuscripts

For Peer Review

SCA28 Cagnoli C

1
2
3
4
5
6
7
8
9
10
11
12
13
14
15
16
17
18
19
20
21

**MISSENSE MUTATIONS IN THE AFG3L2 PROTEOLYTIC DOMAIN
ACCOUNT FOR ~1.5% OF EUROPEAN AUTOSOMAL DOMINANT
CEREBELLAR ATAXIAS**

22
23
24
25
26
27
28
29
30
31
32
33
34
35
36
37
38
39
40

Claudia Cagnoli,^{1,2} Giovanni Stevanin,^{3,4,5,10} Alessandro Brussino,^{1,2} Marco Barberis,^{1,2} Cecilia Mancini,^{1,2} Russell L. Margolis,⁶ Susan E. Holmes,⁶ Marcello Nobili,⁷ Sylvie Forlani,^{3,5} Sergio Padovan,⁸ Patrizia Pappi,² Cécile Zarus,⁵ Isabelle Leber,^{3,5} Pascale Ribai,^{3,4} Luisa Pugliese,⁹ Corrado Assalto,⁹ Alexis Brice,^{3,4,5} Nicola Migone,^{1,2} Alexandra Dürr,^{3,4,5} and Alfredo Brusco^{1,2}

1 Department of Genetics, Biology and Biochemistry, University of Torino

2 S.C. Medical Genetics, A.O.U. San Giovanni Battista, Torino, Italy

3 INSERM, U975 (formerly U679), Paris, France

4 UPMC Univ. Paris 6, UMR_S975, Centre de Recherche de l'Institut du Cerveau et de la Moelle épinière, CNRS 7225, Pitié-Salpêtrière Hospital, 75013 Paris, France

5 APHP, Pitié-Salpêtrière Hospital, Department of Genetics and Cytogenetics, Paris, France

6 Department of Psychiatry and Behavioral Sciences, Johns Hopkins University School of Medicine, Baltimore, Maryland, USA

7 Division of Neurology, Martini Hospital, Turin, Italy

8 IBB-CNR c/o Molecular Biotechnology Center University of Torino, Via Nizza 52, I 10125 Torino, Italy

9 S.A.F.AN. BIOINFORMATICS, Turin (Italy)

10 Ecole Pratique des Hautes Etudes (EPHE), Paris, France

41
42
43
44
45
46
47
48

Correspondence to: Alfredo Brusco, Dipartimento di Genetica Biologia e Biochimica, Università degli Studi di Torino, via Santena 19, 10126, Torino, Italy. Fax +390112366662; e-mail: alfredo.brusco@unito.it

Running title: SCA28 mutations

49
50
51
52
53
54
55
56
57
58
59
60

Paper word count: 5391

SCA28 Cagnoli C

ABSTRACT

Spinocerebellar ataxia type 28 is an autosomal dominant form of cerebellar ataxia (ADCA) caused by mutations in *AFG3L2*, a gene that encodes a subunit of the mitochondrial *m*-AAA protease. We screened 366 primarily Caucasian ADCA families, negative for the most common triplet-expansions, for point mutations in *AFG3L2* using DHPLC. Whole-gene deletions were excluded in 300 of the patients, and duplications were excluded in 129 patients. We found six missense mutations in nine unrelated index cases (9/366, 2.6%): c.1961C>T (p.Thr654Ile) in exon 15, c.1996A>G (p.Met666Val), c.1997T>G (p.Met666Arg), c.1997T>C (p.Met666Thr), c.2011G>A (p.Gly671Arg), and c.2012G>A (p.Gly671Glu) in exon 16. All mutated amino acids were located in the C-terminal proteolytic domain. In available cases, we demonstrated the mutations segregated with the disease. Mutated amino acids are highly conserved, and bioinformatic analysis indicates the substitutions are likely deleterious. This investigation demonstrates that SCA28 accounts for ~3% of ADCA Caucasian cases negative for triplet expansions and, *in extenso*, to ~1.5% of all ADCA. We further confirm both the involvement of *AFG3L2* gene in SCA28 and the presence of a mutational hotspot in exons 15-16. Screening for SCA28, is warranted in patients who test negative for more common SCAs and present with a slowly progressive cerebellar ataxia accompanied by oculomotor signs.

Key Words: Autosomal Dominant Cerebellar Ataxia; Spinocerebellar ataxia; SCA28; AFG3L2; mutation screening

SCA28 Cagnoli C

INTRODUCTION

Autosomal dominant cerebellar ataxias (ADCAs, or SCAs) are a group of clinically heterogeneous neurodegenerative disorders primarily characterized by imbalance, progressive gait and limb ataxia, and dysarthria (Harding, 1993). The clinical phenotype is often complicated by the presence of additional neurological signs, which are highly variable among and within families (Finsterer, 2009; Schols, et al., 2004). SCAs are among the most genetically heterogeneous neurodegenerative diseases, at present nearly thirty genetically distinct subtypes have been defined (<http://www.neuro.wustl.edu/neuromuscular/ataxia/domatax.html>). In most countries, an expansion of a coding CAG-triplet repeat, resulting in production of a protein with an abnormal polyglutamine (polyQ) stretch, accounts for 40-60% of ADCA. In some populations, as in Southern Brazil, founder effects have raised this ratio up to ~100% (Jardim, et al., 2001; Storey, et al., 2000). Less common SCAs are caused by other types of mutations: the expansion of a tri- or penta-nucleotide in untranslated regions (CAG in SCA12, ATTCT in SCA10, and TGGAA in SCA31), by point mutations (SCA5, SCA11, SCA13, SCA14, and SCA27), or by gene dosage anomalies (SCA15 and SCA20) (Fahey, et al., 2005; Holmes, et al., 1999; Houlden, et al., 2007; Ikeda, et al., 2006; Knight, et al., 2008; Matsuura and Ashizawa, 2002; Sato, et al., 2009; van de Leemput, et al., 2007; Waters, et al., 2006). Most recently, point mutations of *AFG3L2* (OMIM #610246) have been shown to cause SCA28 (Di Bella, et al., 2010; Edener, et al., 2010). *AFG3L2* was originally cloned as a paralogue of the *SPG7* gene (encoding for paraplegin, OMIM *602783) (Banfi, et al., 1999), whose loss-of-function causes an autosomal recessive form of hereditary spastic paraplegia (HSP) (Casari, et al., 1998). *AFG3L2* encodes for a subunit of the hetero-oligomeric *m*-AAA protease (ATPases associated with various cellular activities), a component of the mitochondrial ATP-dependent metalloprotease located on the inner mitochondrial membrane. The AAA metalloproteases take part in proteolytic quality control and chaperon-like activities in mitochondria by degrading misfolded proteins and promoting the assembly of respiratory chain complexes (Leonhard, et al., 1999).

Here we examine the prevalence of SCA28 among Caucasian ADCA families, further defining the

SCA28 Cagnoli C

scope and pathogenicity of *AFG3L2* mutations and the clinical features of this disease.

PATIENTS AND METHODS

Patients

We recruited 366 index cases with progressive cerebellar ataxia and a family history of a similar disorder (defined as the presence of at least two affected individuals in at least two consecutive generations). The mean age at onset was 41.1 ± 18.3 years (range: 1-79 years; onset defined as the year of the first symptoms, as reported by the patient or the family). When possible, additional family members were recruited if a mutation in *AFG3L2* was found in a proband. Most patients originated from France (n= 240), but the collection also included patients from other countries in Europe (n= 50), the United States (n =66, predominately of European origin), North-Africa/Middle-East (n= 6), French West-Indies (n= 3) and Madagascar (n= 1). We excluded individuals with pathogenic expansions in the SCA1-3, 6, 7, 17 and DRPLA loci, or recurrent mutations in the SCA5, SCA13, SCA14, or FGF14/SCA27 loci (Klebe, et al., 2005) (Stevanin et al., unpublished data). Clinical and genetic studies were performed after obtaining informed consent from all participants or the parents of participating minors and with the approval of the local ethics committees. Ninety-five French and 95 Italian healthy controls were examined to establish the frequency of variants in the normal population.

Mutation screening

The 17 coding exons of the *AFG3L2* gene (RefSeq NM_006796.1) were PCR amplified using primer and conditions reported in Supp. materials and methods and Supp. Table S1. Mutation analysis was performed on the amplicons using a DHPLC WAVE System (Transgenomics) with melting temperatures (T_m and $T_m+2^\circ\text{C}$) determined by DHPLC Melt software (Jones, et al., 1999) (Supp. Table S1). A normal control profile was always compared with that from a patient. PCR products showing a DHPLC peak shift were purified using the ExoSAP method (MBI-Fermentas,

SCA28 Cagnoli C

1
2
3 Vilnius, Lithuania), and directly sequenced using the Big-Dye terminator cycle sequencing kit ver.
4
5 1.1 and an ABI Prism 3100 Avant automatic sequencer (Applied Biosystems, Foster City, CA). The
6
7 17 coding exons of the *SPG7* gene (RefSeq NM_003119.2) were also amplified and directly
8
9 sequenced following primers and conditions reported in Supp. materials and methods and Supp.
10
11 Table S2.
12
13

14
15 *AFG3L2* gene copy number was evaluated by quantitative duplex PCR (qPCR) using a Roche-UPL
16
17 assay centered on exon 14 (Roche-Diagnostics, Mannheim, Germany). The gene dosage strategy
18
19 was based on the relative amplification of the target sequence (*AFG3L2*) and the co-amplified
20
21 internal standard *RNaseP* using the comparative delta Ct method described elsewhere (Livak and
22
23 Schmittgen, 2001) (see Supp. materials and methods).
24
25

26
27 Nucleotide numbering throughout the paper follows cDNA numbering: +1 refers to the first
28
29 nucleotide of the ATG translation initiation codon of the corresponding RefSeq, according to
30
31 journal guidelines (www.hgvs.org/mutnomen). The initiation codon is codon 1.
32
33

34 35 36 *Haplotype reconstruction*

37
38 Five 6-FAM fluorescently-labelled microsatellites spanning ~10 Mb on chromosome 18, including
39
40 two markers telomeric (*D18S1150* and *D18S53*) and three centromeric (*D18453*, *D18S1104*, and
41
42 *D18S1107*) to *AFG3L2* were genotyped in all available subjects with a specific mutation whenever
43
44 the mutation occurred in at least two unrelated families. We used standard PCR conditions and
45
46 primers described at www.genome.ucsc.edu. Haplotypes were manually reconstructed.
47
48
49

50 51 52 *Homology modeling of AFG3L2, in-silico*

53
54 The three-dimensional model of human AFG3L2 protein was generated using “homology
55
56 modelling”, a bioinformatics algorithm that builds a model of the "target" protein based on the
57
58 homology of its amino acid sequence with that of proteins of known structure (Marti-Renom, et al.,
59
60 2000). The AFG3L2 protein model was constructed with the NEST application (Petrey, et al.,

SCA28 Cagnoli C

1
2
3 2003), using the *T. maritima* FtsH 2CE7 crystal structure as a template (see Supp. materials and
4 methods). Mutations p.Thr654Ile, p.Met666Val, p.Met666Thr, p.Met666Arg, p.Gly671Glu and
5
6 p.Gly671Arg were introduced into the model with the Yasara software (<http://www.yasara.org>) and
7
8 their consequences were evaluated using a series of bioinformatics tools (see also Supp. materials
9
10 and methods).

11
12
13 Multiple species alignment of AFG3L2 protein was made with the ClustalW software
14
15 (<http://www.ebi.ac.uk/Tools/clustalw2/index.html>) using orthologue sequences obtained through
16
17 the Ensembl genome browser (<http://www.ensembl.org>). *In silico* analysis of the possible
18
19 pathogenicity of each amino acid substitution was performed with two different applications: (i)
20
21 PolyPhen (“Polymorphism Phenotyping”, <http://genetics.bwh.harvard.edu/pph/index.html>),
22
23 selecting the Protein Data-Base (PDB) as a source for sequence alignment, and (ii) SIFT (“Sorting
24
25 Intolerant From Tolerant”, <http://blocks.fhcrc.org/sift/>). Possible effects on splicing were checked
26
27 using the applications Splice Site Prediction (http://www.fruitfly.org/seq_tools/splice.html) (Reese,
28
29 et al., 1997), ESEfinder 2.0 (<http://rulai.cshl.edu/tools/ESE/>) (Cartegni, et al., 2003; Smith, et al.,
30
31 2006), and PESXs (<http://cubweb.biology.columbia.edu/pesx/>) (Zhang, et al., 2005). One variant,
32
33 predicted to alter splicing, was further investigated using a minigene assay (see Supp. materials and
34
35 methods).

36 37 38 39 40 41 42 43 44 45 46 **RESULTS**

47 48 *SCA28 mutations in ADCA families.*

49
50 Three-hundred sixty six unrelated patients with ADCA were screened for point mutations in the
51
52 *AFG3L2* gene using DHPLC, followed by direct sequencing of the amplimers with shifted peaks.
53
54 We found six missense changes in nine unrelated index cases: eight were French and one was of
55
56 Italian origin (9/366, 2.6%): c.1961C>T (p.Thr654Ile) in exon 15, c.1996A>G (p.Met666Val),
57
58 c.1997T>G (p.Met666Arg), c.1997T>C (p.Met666Thr), c.2011G>A (p.Gly671Arg) and
59
60 c.2012G>A (p.Gly671Glu) in exon 16 (Figure 1). These mutations were not reported as

SCA28 Cagnoli C

1
2
3 polymorphisms in the dbSNP database build 130 (<http://www.ncbi.nlm.nih.gov/projects/SNP/>), and
4
5 were not found among 380 French or Italian healthy control chromosomes. DNA from 27 additional
6
7 family members in six families was available, which allowed us to verify that the mutation
8
9 segregated with the disease and was absent in healthy relatives (Figure 2). The mutations were
10
11 located in the peptidase-M41 domain of the AFG3L2 protein. Multiple species alignment showed
12
13 that the three amino acids altered by mutations (Thr654, Met666 and Gly671) are conserved
14
15 through *Saccharomyces cerevisiae* (Figure 1). The applications PolyPhen and SIFT predicted that
16
17 all the amino acid mutations are deleterious. Three mutations (p.Thr654Ile, p.Met666Val and
18
19 p.Gly671Arg) were found in two families each. Haplotype reconstruction showed that identical
20
21 mutations shared a common haplotype, suggesting that the families have a common ancestor
22
23 (Figure 2).
24
25
26
27
28

29 In addition to the six missense mutations, we found 25 variants, 14 of which were neither reported
30
31 as polymorphisms in the dbSNP database nor found in healthy controls (Supp. Table S3). Twelve
32
33 were intronic nucleotide changes and two were synonymous substitutions. *In silico* analysis of the
34
35 effect of each variant on splicing showed that c.293-13_293-14delTT changes the score of the exon
36
37 4 acceptor splice site from 0.22 to 0.03. Neither relatives nor cDNA of this patient were available
38
39 for further study. We tested the effect of this mutation using a minigene assay, which showed it has
40
41 no effect on splicing.
42
43
44

45 We also excluded whole-gene deletion/duplication of *AFG3L2* in 129/366 subjects (35%) by qPCR
46
47 of exon 14, and deletions in 171 patients, who carried one or more heterozygous SNP at DHPLC
48
49 and / or direct sequencing.
50
51
52

53
54
55 *3D reconstruction of AFG3L2 and predicted effect of the mutations on intermolecular electrostatic*
56
57 *parameters.*
58

59
60 The three-dimensional reconstruction of the C-terminal region of AFG3L2, the homohexameric
complex, and the relative positions of mutated amino acids are depicted in Figure 3A-B. Based on

SCA28 Cagnoli C

1
2
3 this model, the amino acids Met666 and Gly671 are always on the surface of the complex,
4
5 regardless of the conformation analyzed, suggesting that these two residues may be involved in
6
7 interactions with other molecules. p.Gly671Glu significantly increases the electrostatic potential
8
9 difference between the inner-mitochondrial-membrane side and the matrix side of the hexamer,
10
11 whereas p.Met666Arg and p.Gly671Arg decreased it (Figure 3C and Supp. Table S4). The other
12
13 three mutations do not significantly affect the potential difference (Supp. Table S4). Given that the
14
15 central pore of the *m*-AAA complex (Figure 3D) is used to convey substrates to the proteolytic
16
17 chamber (Kress and Weber-Ban, 2009), we investigated the effect of the mutations of the amino
18
19 acids close to the central pore. As shown in Figure 3E, 3F and Supp. Table S4, p.Gly671Glu
20
21 increases the central pore dipole energy, and p.Met666Arg and p.Gly671Arg decreased it. In
22
23 addition, we found that all the mutations analyzed decreases the mean interaction energy of the
24
25 hexamer, destabilizing the *m*-AAA complex (Supp. Table S5). Taken together, the bioinformatics
26
27 data point to a generalized destabilizing effect of the six mutations detected in our patient
28
29 population, with p.Met666Arg, p.Gly671Glu, and p.Gly671Arg also affecting the charge of the
30
31 hexamer and, in particular, the charge of the translocation channel.
32
33
34
35
36
37
38
39
40

41 *SPG7 mutation analysis*

42
43 Since AFG3L2 and paraplegin can interact to form the multimeric *m*-AAA protease complex, we
44
45 speculated that *SPG7* variants could modify the SCA28 phenotype. We screened for *SPG7* variants
46
47 by direct sequencing the coding exons of nine SCA28 patients with the earliest onset (AAD-080_9,
48
49 AAR-197_1, SAL-872_6, SAL-872_9, SAL-331_11, AAD-444_3, AAD-444_9, AAD-455_19,
50
51 AAD-701_21). Two unreported intronic variants were detected: c.1678+13 C>T in subject 701_21;
52
53 c.2196+18 C>G in subject 331_11. Neither variant is predicted to alter splicing.
54
55
56
57
58
59
60

Clinical features

Table 1 reports the clinical and neuroradiological features of twenty-five SCA28 patients from ten

SCA28 Cagnoli C

1
2
3 families, 14 males and 11 females, clinically examined at a mean age of 45.4 ± 17.7 years (range
4
5 10-77 yrs). The mean age at onset was 30.7 ± 16.2 yrs (range: 6-60 yrs). Cerebellar gait ataxia was
6
7 the initial clinical abnormality in all but one patient (AAR-197_8). At examination, cerebellar
8
9 ataxia was associated with dysarthria (17/25, 68%), ophthalmoplegia (12/25, 48%) and/or gazed-
10
11 evoked nystagmus (13/24, 54%). In addition, saccadic pursuit was noted in 6/16 (37%) and slow
12
13 saccades were present in 3/12 (25%). Ptosis was often present (8/19, 42%) and it was not correlated
14
15 with disease duration ($p= 0.937$). Summing up gazed-evoked nystagmus, ophthalmoplegia and
16
17 ptosis, 19 out of 25 patients had one or more oculomotor anomalies (76%). Six patients had a full
18
19 pyramidal syndrome (i.e., increased reflexes and Babinski sign) and gait spasticity was evident in
20
21 one patient (AAR-197_10), two features already described in SCA28 (Mariotti, et al., 2008).
22
23 Interestingly, extrapyramidal signs, either dystonia ($n=3$) or parkinsonism ($n=3$), were also present
24
25 although relatively infrequent (24%). In patient SAL-872_6, the etiology of parkinsonism may have
26
27 been related to concomitant treatment with a neuroleptic. Vibration sense at the ankles was
28
29 decreased in 9/20 patients (45%), but nerve conduction studies, available for seven patients (five of
30
31 whom had vibration sense alterations) were normal, with neurogenic changes on electromyography
32
33 observed only in SAL-331_4 and SAL-331_11. Two patients from the same family (SAL-331) had
34
35 low verbal IQ (78 and 89, respectively). Cerebral MRI ($n=10$) or CT scan ($n=2$) revealed cerebellar
36
37 atrophy affecting predominantly the vermis. The brainstem was normal. A muscle biopsy performed
38
39 in one patient was unremarkable.
40
41
42
43
44
45
46
47

48 Overall, the disease was slowly progressive and rarely severe. Only patient SAL-444_3 needed help
49
50 for walking, 29 years after the onset of symptoms, and five clinically affected patients of two
51
52 families were not functionally incapacitated (SAL-701_29, SAL-701_021, AAD-080_56, AAD-
53
54 080_57 and AAD-080_58).
55
56
57
58
59
60

DISCUSSION

The *m*-AAA protease is an ATP-dependent proteolytic complex located in the matrix side of the

SCA28 Cagnoli C

1
2
3 inner mitochondrial membrane and involved, in yeast, in protein quality control and protein
4 processing (Arlt, et al., 1996; Esser, et al., 2002; Leonhard, et al., 2000). Human *m*-AAA protease
5 consists of two isoenzymes: (i) a hetero-oligomeric complex formed by paraplegin (SPG7) and
6 AFG3L2, and (ii) a homo-oligomeric AFG3L2 complex. Loss-of-function mutations in the *SPG7*
7 gene cause an autosomal recessive hereditary spastic paraparesis (HSP), whereas *AFG3L2*
8 mutations cause SCA28 (Di Bella, et al., 2010; Edener, et al., 2010). In 366 unrelated ADCA
9 patients of predominately European ancestry, we found nine affected subjects harboring six
10 different *AFG3L2* mutations, clustered in exons 15 (p.Thr654Ile) and 16 (p.Met666Arg,
11 p.Met666Thr, p.Met666Val, p.Gly671Arg and p.Gly671Gln). The pathogenicity of these missense
12 substitutions is supported by multiple lines of evidence: (i) in families where more than one affected
13 subject was available, we demonstrated that the mutation segregated with the disease and was not
14 present in healthy subjects of the family. In one of these families (AAD-080), a positive multipoint
15 LOD score of 2.54 at D18S853 highly suggested its linkage to the SCA28 locus (data not shown).
16 Moreover, STR-analysis revealed that patients from different families harboring the same mutation
17 shared a common haplotype, suggesting the presence of common ancestors. (ii) Mutations were not
18 found in 380 control chromosomes. (iii) The mutated amino acids are evolutionary conserved up to
19 the *S. cerevisiae* orthologous protein Yta10, and all are located in the M41-proteolytic domain of
20 the protein. (iv) Bioinformatic analysis of the protein showed that the mutations alter the interaction
21 of each monomer with the other five, symptomatic of an altered stability of the complex. Yeast
22 complementation studies, beyond the scope of this investigation, would further establish the
23 functional significance of these mutations.
24
25
26
27
28
29
30
31
32
33
34
35
36
37
38
39
40
41
42
43
44
45
46
47
48
49
50
51

52 The *m*-AAA mechanism of action is still under study, although recent investigations of its bacterial
53 homologue FtsH indicate that the protease ring is stationary and that coordinated ATP-driven
54 movements of each monomer accomplish substrate unfolding and translocation to the proteolytic
55 chamber (Augustin, et al., 2009; Bieniossek, et al., 2009). The electrostatic potential difference of
56 the complex and the dipole of the central pore are altered in three of the six mutations that we
57
58
59
60

SCA28 Cagnoli C

1
2
3 detected. Furthermore, all six mutations diminish the interaction energy among monomers. These
4
5 effects of the mutations suggest that each may have a negative effect on the *m*-AAA complex
6
7 activity. For instance, the capacity of the complex to move substrates towards the proteolytic
8
9 chamber through ATPase activity may be impaired by weaker interaction among monomers or by
10
11 abnormal electrostatic potentials through the central pore (Striebel, et al., 2009).
12
13

14
15 Five of the six *AFG3L2* missense mutations previously reported, cluster in the proteolytic domain at
16
17 amino acids Ser674, Glu691, Ala694, Glu700, and Arg702 (exon 16) (Di Bella, et al., 2010;
18
19 Edener, et al., 2010). We found different mutations affecting the same amino acids (p.Gly671Arg
20
21 and p.Gly671Glu; p.Met666Arg, p.Met666Thr, and p.Met666Val) indicating that exons 15 and 16
22
23 are mutational hotspots for SCA28, and consistent with the hypothesis that disruption of the
24
25 peptidase domain is critical to the pathogenesis of SCA28.
26
27

28
29 Recent evidences from animal models also support the pathogenicity of *AFG3L2* mutations: *Afg3l2*
30
31 knock-out mice presents with a severe neuromuscular phenotype, caused by a defect in motor axon
32
33 and cerebellar development (Maltecca, et al., 2008), whereas the *Afg3l2*^{Emv66} mouse, carrying a
34
35 heterozygous loss-of-function mutation, develops a phenotype with similarities to SCA28
36
37 (Maltecca, et al., 2009). Whole gene deletions were excluded in 300/366 patients and duplications
38
39 in 129/366, suggesting that *AFG3L2* deletions/duplications are not common in ADCAs. Moreover,
40
41 two related patients with an 18p deletion encompassing *AFG3L2* reportedly have not developed
42
43 ataxia (Nasir, et al., 2006). Copy number variants encompassing part or whole of *AFG3L2* gene
44
45 exist in normal individuals (Kim, et al., 2009; Redon, et al., 2006). Therefore, in addition to the
46
47 results of our screening designed to detect only large deletions and duplications, the absence of a
48
49 phenotype in humans with duplications and deletions affecting *AFG3L2*, and the different
50
51 phenotype observed in *Afg3l2* null mice compared to *Afg3l2*^{Emv66} mice, suggest that heterozygous
52
53 deletions or duplications of the *AFG3L2* gene may not cause SCA28. Looking at rearrangements in
54
55 SCA28 should therefore not be prescribed in clinical practice.
56
57
58
59
60

Our survey shows that SCA28 is rare among European ADCA patients, accounting for ~3% of the

SCA28 Cagnoli C

1
2
3 analyzed cases and ~1.5% of all ADCAs. As a comparison, polyglutamine expansions account for
4
5 about 50%. The clinical and neuroradiological phenotype of the newly ascertained families is
6
7 similar to that of the SCA28 patients reported so far (Cagnoli, et al., 2006; Edener, et al., 2010;
8
9 Mariotti, et al., 2008): disease onset is in adulthood and the disease progresses slowly with
10
11 preserved functional capacity, decades after the diagnosis. The mean age at onset and age at onset
12
13 variability is similar in our series and in the reported families: in five patients the onset was above
14
15 50 yrs, whereas two subjects were symptomatic at 6 and 8 yrs. Even in the young onset cases, the
16
17 disease progressed relatively slowly, a much different pattern than has been observed in the
18
19 polyglutamine diseases and evidence that SCA28 is not caused by cryptic polyglutamine expansion.
20
21 Interestingly, extrapyramidal features were not rare in our series of patients in contrast to previous
22
23 reports, of potential value in speculating on the clinical diagnosis prior to genetic testing. As in
24
25 many genetic diseases, particularly in those affecting the nervous system, the extent to which
26
27 environmental factors affect disease phenotype, including onset age, selective neuronal
28
29 involvement, and disease progression, remains to be determined.
30
31
32
33
34

35
36 Given the signs and symptoms of the disease, we suggest that the diagnosis of SCA28 should be
37
38 considered in the presence of slowly progressive ataxia associated with oculomotor abnormalities.
39
40 So far, *AFG3L2* mutations seem to cluster in exons 10, 15, and 16, which should facilitate genetic
41
42 diagnosis in clinical practice and a better understanding of the function and malfunction of
43
44 *AFG3L2*.
45
46
47
48
49

50 **Acknowledgments.**

51
52 We are grateful to the family members for their participation, to the DNA and Cell bank of the
53
54 Centre de Recherche de l'Institut du Cerveau et de la Moelle épinière for technical assistance and to
55
56 Drs C Marelli, J Yaouang, M Ponsot, H Chneiweiss, D Ménard, S Schaeffer, A Lagueny, L Carluer
57
58 and Y Boukhriché as well as Prof A Harding for referring some of the patients and for clinical
59
60 examinations.

SCA28 Cagnoli C

This work was funded by Telethon Research grant GGP07110 (to A Brusco), Regione Piemonte Ricerca Sanitaria Finalizzata, the European Union (to the EUROSCA consortium), the VERUM foundation (to A Brice) and the Programme Hospitalier de Recherche Clinique (to A Durr).

For Peer Review

1
2
3
4
5
6
7
8
9
10
11
12
13
14
15
16
17
18
19
20
21
22
23
24
25
26
27
28
29
30
31
32
33
34
35
36
37
38
39
40
41
42
43
44
45
46
47
48
49
50
51
52
53
54
55
56
57
58
59
60

SCA28 Cagnoli C

FIGURE LEGENDS

Figure 1.

Localization of the six *AFG3L2* missense mutations. In the upper panel the amino acid alignment of the *AFG3L2* protein corresponding to a region including a portion of exons 15 and 16 is shown for 13 orthologous proteins from *H. sapiens* to *S. cerevisiae*. The mutated amino acids Thr654, Met666 and Gly671 are highlighted. Below, a scheme of the *AFG3L2* genomic region and the protein are shown. Domain names are: MTS: mitochondrial targeting signal; TM: transmembrane domain; FtsH: Filamentation temperature sensitive H proteolytic domain; AAA: ATPase Associated with different cellular activities.

Figure 2.

Pedigrees of the nine families segregating a *AFG3L2* mutation. Square and circles shadings: white = healthy; black = SCA28; gray = presumed SCA28; hash = asymptomatic subject carrying a disease haplotype. Five STR markers (on the left) were used to reconstruct the SCA28-surrounding haplotype that suggest a common ancestor for p.Thr541Ile, p.Met666Val and p.Gly671Arg mutations, in two families each. All subjects whose DNA was available (hyphen above the symbol) were tested for the *AFG3L2* mutation segregating in the family.

Figure 3.

Bioinformatics analysis of *AFG3L2* missense changes. Panel A, monomeric structure of the *AFG3L2* protein, with the localization of ATP (yellow), the Zn^{++} ion (pink) and the three mutated amino acids, Thr541 (light blue), Met666 (dark blue) and Gly671 (green). Panel B, matrix-side view of *AFG3L2* hexamer (see panel A for color-code of Zn^{++} and mutated amino acids); a dotted line shows the cross-section level of panel C. Panel C, electrostatic potential at the surface of the *AFG3L2* hexamer viewed from the matrix side (upper row) and from the IMM side (lower row) is

SCA28 Cagnoli C

1
2
3 reported for the mutations changing the potential difference. The mutation analyzed is reported
4
5 between the images of the two surfaces; blue = positive charges, red = negative charges; the black
6
7 box identifies the central pore magnified in panels E (membrane side) and F (matrix side). In panels
8
9 E and F only the charges of the amino acids closer than 10 Å from the geometric center of the
10
11 dipole are shown. Panel D, side-view of the hexamer with the localization of the central
12
13 translocation channel colored (blue = positive charges, red = negative charges); wt = wild-type;
14
15 IMM = inner mitochondrial membrane.
16
17
18
19
20
21
22
23
24
25
26
27
28
29
30
31
32
33
34
35
36
37
38
39
40
41
42
43
44
45
46
47
48
49
50
51
52
53
54
55
56
57
58
59
60

For Peer Review

SCA28 Cagnoli C

REFERENCES

- Arlt H, Tauer R, Feldmann H, Neupert W, Langer T. 1996. The YTA10-12 complex, an AAA protease with chaperone-like activity in the inner membrane of mitochondria. *Cell* 85(6):875-85.
- Atorino L, Silvestri L, Koppen M, Cassina L, Ballabio A, Marconi R, Langer T, Casari G. 2003. Loss of m-AAA protease in mitochondria causes complex I deficiency and increased sensitivity to oxidative stress in hereditary spastic paraplegia. *J Cell Biol* 163(4):777-87.
- Augustin S, Gerdes F, Lee S, Tsai FT, Langer T, Tatsuta T. 2009. An intersubunit signaling network coordinates ATP hydrolysis by m-AAA proteases. *Mol Cell* 35(5):574-85.
- Banfi S, Bassi MT, Andolfi G, Marchitello A, Zanotta S, Ballabio A, Casari G, Franco B. 1999. Identification and characterization of AFG3L2, a novel paraplegin-related gene. *Genomics* 59(1):51-8.
- Bieniossek C, Niederhauser B, Baumann UM. 2009. The crystal structure of apo-FtsH reveals domain movements necessary for substrate unfolding and translocation. *Proc Natl Acad Sci U S A* 106(51):21579-84.
- Cagnoli C, Mariotti C, Taroni F, Seri M, Brussino A, Michielotto C, Grisoli M, Di Bella D, Migone N, Gellera C and others. 2006. SCA28, a novel form of autosomal dominant cerebellar ataxia on chromosome 18p11.22-q11.2. *Brain* 129(Pt 1):235-42.
- Cartegni L, Wang J, Zhu Z, Zhang MQ, Krainer AR. 2003. ESEfinder: A web resource to identify exonic splicing enhancers. *Nucleic Acids Res* 31(13):3568-71.
- Casari G, De Fusco M, Ciarmatori S, Zeviani M, Mora M, Fernandez P, De Michele G, Filla A, Coccozza S, Marconi R and others. 1998. Spastic paraplegia and OXPHOS impairment caused by mutations in paraplegin, a nuclear-encoded mitochondrial metalloprotease. *Cell* 93(6):973-83.
- Di Bella D, Lazzaro F, Brusco A, Plumari M, Battaglia G, Pastore A, Finardi A, Cagnoli C, Tempia F, Frontali M and others. 2010. Mutations in the mitochondrial protease gene AFG3L2 cause dominant hereditary ataxia SCA28. *Nat Genet* 42(4).
- Edener U, Wollner J, Hehr U, Kohl Z, Schilling S, Kreuz F, Bauer P, Bernard V, Gillessen-Kaesbach G, Zuhlke C. 2010. Early onset and slow progression of SCA28, a rare dominant ataxia in a large four-generation family with a novel AFG3L2 mutation. *Eur J Hum Genet*.
- Esser K, Tursun B, Ingenhoven M, Michaelis G, Pratje E. 2002. A novel two-step mechanism for removal of a mitochondrial signal sequence involves the mAAA complex and the putative rhomboid protease Pcp1. *J Mol Biol* 323(5):835-43.
- Fahey MC, Knight MA, Shaw JH, Gardner RJ, du Sart D, Lockhart PJ, Delatycki MB, Gates PC, Storey E. 2005. Spinocerebellar ataxia type 14: study of a family with an exon 5 mutation in the PRKCG gene. *J Neurol Neurosurg Psychiatry* 76(12):1720-2.
- Finsterer J. 2009. Ataxias with autosomal, X-chromosomal or maternal inheritance. *Can J Neurol Sci* 36(4):409-28.
- Gilis D, Rooman M. 2000. PoPMuSiC, an algorithm for predicting protein mutant stability changes: application to prion proteins. *Protein Eng* 13(12):849-56.
- Guerois R, Nielsen JE, Serrano L. 2002. Predicting changes in the stability of proteins and protein complexes: a study of more than 1000 mutations. *J Mol Biol* 320(2):369-87.
- Harding AE. 1993. Clinical features and classification of inherited ataxias. New York: Raven Press.
- Holmes SE, O'Hearn EE, McInnis MG, Gorelick-Feldman DA, Kleiderlein JJ, Callahan C, Kwak NG, Ingersoll-Ashworth RG, Sherr M, Sumner AJ and others. 1999. Expansion of a novel CAG trinucleotide repeat in the 5' region of PPP2R2B is associated with SCA12. *Nat Genet* 23(4):391-2.
- Houlden H, Johnson J, Gardner-Thorpe C, Lashley T, Hernandez D, Worth P, Singleton AB, Hilton DA, Holton J, Revesz T and others. 2007. Mutations in TTBK2, encoding a kinase

SCA28 Cagnoli C

- 1
2
3 implicated in tau phosphorylation, segregate with spinocerebellar ataxia type 11. *Nat Genet*
4 39(12):1434-6.
- 5
6 Ikeda Y, Dick KA, Weatherspoon MR, Gincel D, Armbrust KR, Dalton JC, Stevanin G, Durr A,
7 Zuhlke C, Burk K and others. 2006. Spectrin mutations cause spinocerebellar ataxia type 5.
8 *Nat Genet* 38(2):184-90.
- 9
10 Jardim LB, Silveira I, Pereira ML, Ferro A, Alonso I, do Ceu Moreira M, Mendonca P, Ferreirinha
11 F, Sequeiros J, Giugliani R. 2001. A survey of spinocerebellar ataxia in South Brazil - 66
12 new cases with Machado-Joseph disease, SCA7, SCA8, or unidentified disease-causing
13 mutations. *J Neurol* 248(10):870-6.
- 14
15 Jones AC, Austin J, Hansen N, Hoogendoorn B, Oefner PJ, Cheadle JP, O'Donovan MC. 1999.
16 Optimal temperature selection for mutation detection by denaturing HPLC and comparison
17 to single-stranded conformation polymorphism and heteroduplex analysis. *Clin Chem* 45(8
18 Pt 1):1133-40.
- 19
20 Jung J, Lee B. 2000. Protein structure alignment using environmental profiles. *Protein Eng*
21 13(8):535-43.
- 22
23 Kim KY, Lee GY, Kim J, Jeung HC, Chung HC, Rha SY. 2009. Identification of significant
24 regional genetic variations using continuous CNV values in aCGH data. *Genomics*
25 94(5):317-23.
- 26
27 Klebe S, Durr A, Rentschler A, Hahn-Barma V, Abele M, Bouslam N, Schols L, Jedynek P, Forlani
28 S, Denis E and others. 2005. New mutations in protein kinase Cgamma associated with
29 spinocerebellar ataxia type 14. *Ann Neurol* 58(5):720-9.
- 30
31 Knight MA, Hernandez D, Diede SJ, Dauwerse HG, Rafferty I, van de Leemput J, Forrest SM,
32 Gardner RJ, Storey E, van Ommen GJ and others. 2008. A duplication at chromosome
33 11q12.2-11q12.3 is associated with spinocerebellar ataxia type 20. *Hum Mol Genet*
34 17(24):3847-53.
- 35
36 Kress W, Weber-Ban E. 2009. The alternating power stroke of a 6-cylinder AAA protease
37 chaperone engine. *Mol Cell* 35(5):545-7.
- 38
39 Krieger E, Darden T, Nabuurs SB, Finkelstein A, Vriend G. 2004. Making optimal use of empirical
40 energy functions: force-field parameterization in crystal space. *Proteins* 57(4):678-83.
- 41
42 Leonhard K, Guiard B, Pellicchia G, Tzagoloff A, Neupert W, Langer T. 2000. Membrane protein
43 degradation by AAA proteases in mitochondria: extraction of substrates from either
44 membrane surface. *Mol Cell* 5(4):629-38.
- 45
46 Leonhard K, Stiegler A, Neupert W, Langer T. 1999. Chaperone-like activity of the AAA domain
47 of the yeast Yme1 AAA protease. *Nature* 398(6725):348-51.
- 48
49 Livak KJ, Schmittgen TD. 2001. Analysis of relative gene expression data using real-time
50 quantitative PCR and the 2(-Delta Delta C(T)) Method. *Methods* 25(4):402-8.
- 51
52 Maltecca F, Aghaie A, Schroeder DG, Cassina L, Taylor BA, Phillips SJ, Malaguti M, Previtali S,
53 Guenet JL, Quattrini A and others. 2008. The mitochondrial protease AFG3L2 is essential
54 for axonal development. *J Neurosci* 28(11):2827-36.
- 55
56 Maltecca F, Magnoni R, Cerri F, Cox GA, Quattrini A, Casari G. 2009. Haploinsufficiency of
57 AFG3L2, the gene responsible for spinocerebellar ataxia type 28, causes mitochondria-
58 mediated Purkinje cell dark degeneration. *J Neurosci* 29(29):9244-54.
- 59
60 Mariotti C, Brusco A, Di Bella D, Cagnoli C, Seri M, Gellera C, Di Donato S, Taroni F. 2008.
Spinocerebellar ataxia type 28: a novel autosomal dominant cerebellar ataxia characterized
by slow progression and ophthalmoparesis. *Cerebellum* 7(2):184-8.
- Marti-Renom MA, Stuart AC, Fiser A, Sanchez R, Melo F, Sali A. 2000. Comparative protein
structure modeling of genes and genomes. *Annu Rev Biophys Biomol Struct* 29:291-325.
- Matsuura T, Ashizawa T. 2002. Spinocerebellar ataxia type 10: a disease caused by a large ATTCT
repeat expansion. *Adv Exp Med Biol* 516:79-97.
- Nasir J, Frima N, Pickard B, Malloy MP, Zhan L, Grunewald R. 2006. Unbalanced whole arm
translocation resulting in loss of 18p in dystonia. *Mov Disord* 21(6):859-63.

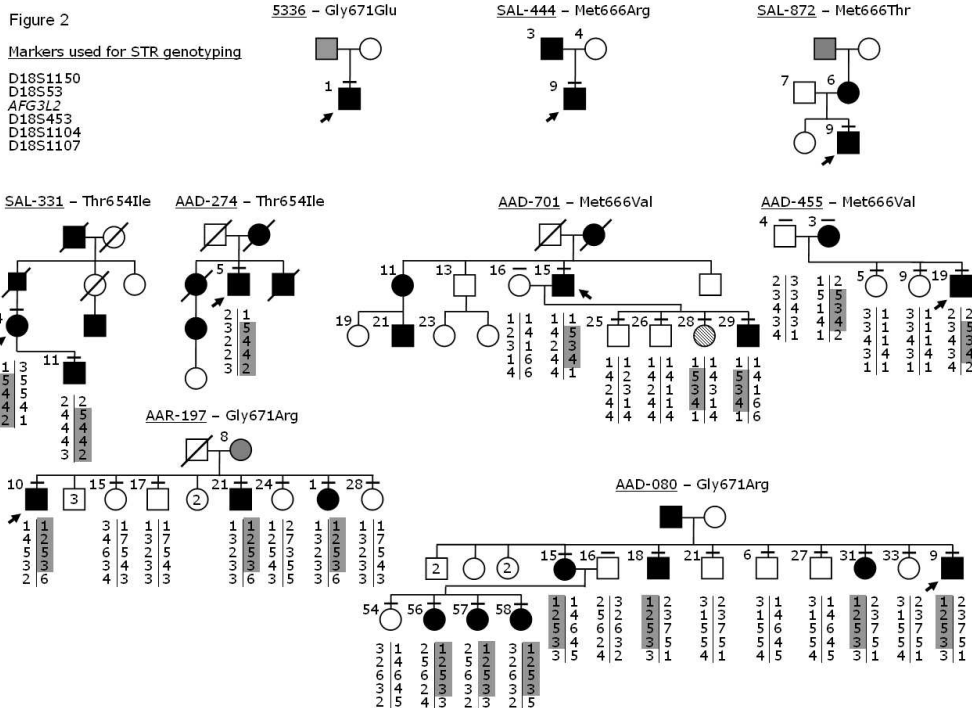
SCA28 Cagnoli C

- 1
2
3 Petrey D, Xiang Z, Tang CL, Xie L, Gimpelev M, Mitros T, Soto CS, Goldsmith-Fischman S,
4 Kernytsky A, Schlessinger A and others. 2003. Using multiple structure alignments, fast
5 model building, and energetic analysis in fold recognition and homology modeling. *Proteins*
6 53 Suppl 6:430-5.
7
8 Redon R, Ishikawa S, Fitch KR, Feuk L, Perry GH, Andrews TD, Fiegler H, Shapero MH, Carson
9 AR, Chen W and others. 2006. Global variation in copy number in the human genome.
10 *Nature* 444(7118):444-54.
11
12 Reese MG, Eeckman FH, Kulp D, Haussler D. 1997. Improved splice site detection in Genie. *J*
13 *Comput Biol* 4(3):311-23.
14
15 Sato N, Amino T, Kobayashi K, Asakawa S, Ishiguro T, Tsunemi T, Takahashi M, Matsuura T,
16 Flanigan KM, Iwasaki S and others. 2009. Spinocerebellar ataxia type 31 is associated with
17 "inserted" penta-nucleotide repeats containing (TGGAA)_n. *Am J Hum Genet* 85(5):544-57.
18
19 Schols L, Bauer P, Schmidt T, Schulte T, Riess O. 2004. Autosomal dominant cerebellar ataxias:
20 clinical features, genetics, and pathogenesis. *Lancet Neurol* 3(5):291-304.
21
22 Smith PJ, Zhang C, Wang J, Chew SL, Zhang MQ, Krainer AR. 2006. An increased specificity
23 score matrix for the prediction of SF2/ASF-specific exonic splicing enhancers. *Hum Mol*
24 *Genet* 15(16):2490-508.
25
26 Storey E, du Sart D, Shaw JH, Lorentzos P, Kelly L, McKinley Gardner RJ, Forrest SM, Biros I,
27 Nicholson GA. 2000. Frequency of spinocerebellar ataxia types 1, 2, 3, 6, and 7 in
28 Australian patients with spinocerebellar ataxia. *Am J Med Genet* 95(4):351-7.
29
30 Striebel F, Kress W, Weber-Ban E. 2009. Controlled destruction: AAA+ ATPases in protein
31 degradation from bacteria to eukaryotes. *Curr Opin Struct Biol* 19(2):209-17.
32
33 van de Leemput J, Chandran J, Knight MA, Holtzclaw LA, Scholz S, Cookson MR, Houlden H,
34 Gwinn-Hardy K, Fung HC, Lin X and others. 2007. Deletion at ITPR1 underlies ataxia in
35 mice and spinocerebellar ataxia 15 in humans. *PLoS Genet* 3(6):e108.
36
37 Vriend G. 1990. WHAT IF: a molecular modeling and drug design program. *J Mol Graph* 8(1):52-
38 6, 29.
39
40 Waters MF, Minassian NA, Stevanin G, Figueroa KP, Bannister JP, Nolte D, Mock AF, Evidente
41 VG, Fee DB, Muller U and others. 2006. Mutations in voltage-gated potassium channel
42 KCNC3 cause degenerative and developmental central nervous system phenotypes. *Nat*
43 *Genet* 38(4):447-51.
44
45 Zhang XH, Kangsamaksin T, Chao MS, Banerjee JK, Chasin LA. 2005. Exon inclusion is
46 dependent on predictable exonic splicing enhancers. *Mol Cell Biol* 25(16):7323-32.
47
48
49
50
51
52
53
54
55
56
57
58
59
60

Table 1. Clinical features of SCA28 patients.

Subject	Mut	Sex	Yrs at Onset	Yrs at Exam	Disease duration (yr)	Functional handicap	Cerebellar Signs					Ophthalmoplegia	LL Reflexes	Ptosis	Bilateral extensor plantar response	Other signs
							Gait ataxia	Limb ataxia	Dysarthria	Horizontal gaze-evoked nystagmus						
SAL-331_4	T654I	F	20	66	46	Moderate	Mild	Mild	none	no	no	+	NA	no	IQ89	
SAL-331_11	T654I	M	10	43	33	Moderate	Moderate	Moderate	Severe	Yes	no	+	NA	no	Dystonic head tremor, IQ78	
AAD-274_5	T654I	M	60	73	13	Moderate	Mild	Mild	Mild	NA	no	+	NA	unilateral	Parkinsonism	
SAL-872_9	M666T	M	20	25	5	Moderate	Moderate	Mild	Moderate	Yes	no	N	no	no	Head tremor, cognitive difficulties	
SAL-872_6	M666T	F	NA	53	NA	Moderate	Moderate	Moderate	Severe	Yes	Vertical	N	NA	no	Severe depression, UL rigidity	
AAD-455_19	M666V	M	28	39	11	Mild	Mild	Mild	Mild	no	Vertical horizontal	N	no	no	-	
AAD-455_3	M666V	F	50	77	27	Moderate	Severe	Mild	Moderate	Yes	Vertical, horizontal	+	Yes	Yes	-	
AAD-701_11	M666V	F	50	61	11	Mild	Mild	Mild	Mild	no	no	N	no	no	UL dystonia	
AAD-701_15	M666V	M	25	58	33	Mild	Moderate	Moderate	Moderate	Yes	Vertical	+	Yes	no	-	
AAD-701_29	M666V	M	20	30	10	none	Mild	Moderate	Moderate	no	no	+	no	unilateral	-	
AAD-701_21	M666V	M	14	38	24	none	Mild	Mild	none	Yes	no	+	no	unilateral	-	
AAD-444_3	M666R	M	8	37	29	Severe	Moderate	Severe	Moderate	Yes	Horizontal	+	no	Yes	Memory difficulties	
AAD-444_9	M666R	M	6	10	4	Mild	Mild	Mild	none	no	no	N	no	no	Behaviour problems	
AAD-080_15	G671R	F	28	50	22	Moderate	Moderate	Moderate	Moderate	no	Vertical, horizontal	+	Yes	no	-	
AAD-080_56	G671R	F	NA	29	NA	none	Mild	Mild	none	Yes	no	+	no	no	-	
AAD-080_57	G671R	F	NA	29	NA	none	Mild	Mild	none	Yes	no	+	no	no	-	
AAD-080_58	G671R	F	NA	25	NA	none	Mild	Mild	none	Yes	no	+	no	no	-	
AAD-080_18	G671R	M	44	49	5	Mild	Mild	Moderate	none	no	Vertical, horizontal	N	Yes	no	-	
AAD-080_31	G671R	F	34	39	5	Moderate	Moderate	Moderate	Moderate	no	no	+	Yes	no	-	
AAD-080_9	G671R	M	23	29	6	Moderate	Moderate	Moderate	Moderate	Yes	Vertical, horizontal	+	NA	no	-	
AAR-197_1	G671R	F	32	36	4	Moderate	Moderate	Moderate	Mild	no	no	+	no	no	-	
AAR-197_10	G671R	M	25	51	26	Moderate	Moderate	Moderate	Moderate	no	Vertical, horizontal	+	Yes	no	Cognitive difficulties, spasticity	
AAR-197_21	G671R	M	39	43	4	Moderate	Moderate	Moderate	Mild	Yes	Vertical, horizontal	NA	Yes	no	-	
AAR-197_8	G671R	F	53	73	20	Moderate	none	none	none	no	Vertical, horizontal	N	Yes	no	Neck dystonia, Parkinsonism	
5336_1	G671E	M	55	71	16	Severe	Severe	Severe	Severe	Yes	no	+	no	Yes	-	

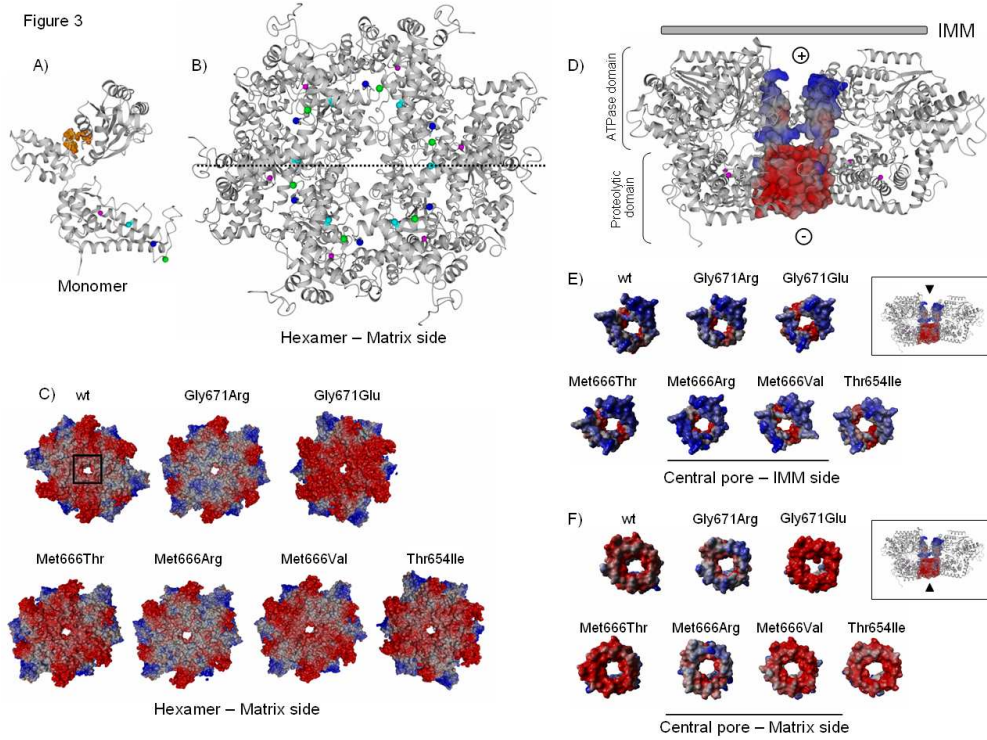
Notes: LL, lower limbs; UL, upper limbs; N, normal; +, augmented; NA, not available;



451x361mm (72 x 72 DPI)

view

1
2
3
4
5
6
7
8
9
10
11
12
13
14
15
16
17
18
19
20
21
22
23
24
25
26
27
28
29
30
31
32
33
34
35
36
37
38
39
40
41
42
43
44
45
46
47
48
49
50
51
52
53
54
55
56
57
58
59
60



451x361mm (72 x 72 DPI)

view

SUPPLEMENTARY MATERIALS AND METHODS.*Mutation screening.*

The 17 coding exons of the *AFG3L2* gene were PCR amplified in a total volume of 50 μ l using 30 ng of genomic DNA, 144 μ M dNTPs, 2 mM MgCl₂, 1 U of Taq Gold (Applied Biosystems, Foster City, CA, USA) and 200 nM of forward and reverse primers reported in supplementary table S1.

The amplification of exon 1 required a final concentration of 1 M betaine (B0300, Sigma-Aldrich, St.Louis, MO, USA). Thermal cycling conditions were: 7 min at 95°C, followed by 14 cycles of 30 sec at 95°C, 30 sec at annealing temperature (Ta)+7°C-0.5°C/cycle (see supplementary table 1 and 1 min at 72°C; then 30 cycles consisting of X mn at 95°C, 30 sec at Ta (see supplementary table S1), and 1 min at 72°C. A final step of 40 cycles consisting of 1 min at 98°C-1°C/cycle was added in case of DHPLC analysis to increment heteroduplex formation.

The 17 coding exons of the *SPG7* gene were amplified and directly sequenced. PCR was performed in a total volume of 25 μ l, using 30 ng of genomic DNA, 144 μ M dNTPs, 2.5 mM MgCl₂, 0.5 U of Taq Gold (Applied Biosystems) and 200 nM of forward and reverse primers reported in supplementary table S2. The amplification of exon 1 required a final concentration of 1 M betaine. Thermal cycling conditions for exons 1-13 were: 7 min at 95°C, followed by 14 cycles of 30 sec at 95°C, 30 sec at Ta+7°C-0.5°C/cycle (see supplementary table 2 and 1 min at 72°C; then 30 cycles consisting in X mn at 95°C, 30 sec at Ta, and 1 min at 72°C; with a final extension for 10 min at 72°C. Thermal cycling conditions for exons 14-17 were: 7 min at 95°C, 30 cycles at 95°C, 30 sec at Ta, and 1 min at 72°C; final extension for 10 min at 72°C. Fragments were purified using the ExoSAP method (MBI-Fermentas), and directly sequenced using the Big-Dye cycle sequencing kit and an ABI Prism 3100 Avant automatic sequencer (Applied Biosystems).

Minigene assay.

A minigene assay was set up to test the effect of *AFG3L2* c.293-13_293-14delTT sequence variant on splicing. We amplified a 327 bp fragment from a subject carrying the variant. The forward

1
2
3 primer (5'-ATGCGAATTCTTGTATTCTTTCTCATAGTGCTTCA) introduced a *EcoRI*
4
5 restriction site, and the reverse primer (5'-TACGTCTAGAAATGCCTCCCAACCTTCTCT)
6
7 introduced a *XbaI* restriction site. The fragment was sequenced to exclude the presence of PCR-
8
9 introduced mutations. The PCR product was cloned into a pTZ57R/T vector using the InsTA
10
11 Cloning kit (Invitrogen), and transformed in DH5 α bacterial cells following manufacturer's
12
13 recommendations (RBC Bioscience, Chung Ho City, Taiwan). Plasmids were extracted using
14
15 standard methods, checked by sequencing, and digested with *EcoRI* and *XbaI* restriction
16
17 endonucleases. The insert was gel-purified and sub-cloned into a pAltermax modified vector
18
19 (kindly provided by dr. Gareth Eldvige, Wellcome Trust Centre, Oxford, UK, and dr. Ivana
20
21 Kurelac, University of Bologna). Plasmids containing the wild-type or the variant sequence were
22
23 used to transform HEK293 cells using the TurboFect kit (Fermentas). After 48h, RNA was
24
25 extracted with the RNeasy Kit (Qiagen), retrotranscribed with the GoScript kit (Promega). The
26
27 cDNA was amplified and sequenced with vector primers.
28
29
30
31
32
33
34
35
36
37
38
39
40
41
42
43
44
45
46
47
48
49
50
51
52
53
54
55
56
57
58
59
60

Supp. Table S1. Primers, PCR and DHPLC conditions for *AFG3L2* mutation screening

Exon	Primers (Forward/Reverse)	PCR Ta (°C)	DHPLC Tm (°C) ¹
1	5'-GTTGAGAGCTTGGGCTCCTCCGTGA 5'-CCAGTGACCTTGACGTCCGCTCTCC	69	68/69/69.8
2	5'-TTATGACCAGGAAATGAAGC 5'-GGTTGGGTCTTTTGTCTCCTT	59	52.3/ 57.3
3	5'-GATGCATCAGCTGCTTTGAA 5'-GGTAGTTTCCACTGAACAAAG	55	53.8
4	5'-GCTGAGAGAGCTAAAACCTTGC 5'-AGAGAAGGTTGGGAGGCATT	55	58.5/60.0/62.0
5	5'-AGAGAAGGTTGGGAGGCATT 5'-ACCAAAGAAGTGACAGTCAGC	55	56.0/58.0/60.0
6	5'-TGAGCTTAAAAGAGTATCTCAAGTATTTT 5'-TGAGGCAGGTTTTCTTTCA	56	52.4/53.4/57.0/58.8
7	5'-TTGAACCGTTTAGTGAATTGAACC 5'-GAACCACAGGCAGCACAGTC	56	53.3/55.7/58.1
8	5'-GAAAGCTGGAGGTGAGCAG 5'-GAGGATCGTTTTGGGTCA	55	55.5/57.5/61.8
9	5'-TGTGGATACACAATTTACTTTTCTGGA 5'-GTGCCTCCATCTGTGGTGAA	56	52.2/69.4/62.0
10	5'-CCGATTTATTTCAATTTCTTATTCAGAG 5'-GCCTGGACGACAGAGTCA	56	56.4/58.0/60.8
11	5'-GCTATGAATTTGCAGTGCTC 5'-AGGTCCAGTGCTCATGAGTG	57	n.a. ²
12	5'-AGGTCCAGTGCTCATGAGTG 5'-TTCTTTACTGTGGGCTTCTT	57	55.6/57.6
13	5'-GATCAGTTTGGGCGTATTTTCG 5'-AATCCCTGGCCTCAAATTCA	56	55.5/57.5/58.4
14	5'-TTGTGATAGGCAGCTCAGTC 5'-CAAGCTACACTCCTGCAAAG	57	56.8/61.5/63.0
15	5'-GTCTTCATCTGTAGTAGGATCTTCAA 5'-CGTGCAAATATGAATACATGAGG	56	55.8/56.8
16	5'-GATTTTGTCTGGTTAAAGAACAATCA 5'-CCAACAAAACAGTCTATCTATCACTTC	56	53.0/56.1/57.8
17	5'-GACTTTGCTGAGTAACTGTATTTAATG 5'-ATGCACCAGCTGAAACCACA	56	53.6/57.2/60.5

Notes: n.a.: not applicable; ¹ as determined by DHPLC Melt software; ² *AFG3L2* exon 11 was directly sequenced in all subjects. Ta=annealing temperature; *AFG3L2* RefSeq NM_006796.1

Supp. Table S2. Primers and PCR conditions for SPG7 mutation screening.
Ta=annealing temperature

Exon	Primers (Forward/Reverse)	Ta (°C)
1	5'-CGCAGGCGCCACGTCAGA 5'-GCCGGGCTGGGCCTTACAGA	63
2	5'-TGTTACCTAAAGCTTTGACCTATTGC 5'-GCTCTGATCACACCATTGTACTGC	58
3	5'-ACACTGTTGTCCTGTATGCCTCC 5'-TCCAGACTGGTTTCACCTTGCTA	58
4	5'-GATGTCGCCCCGTGTCTGTTG 5'-CCACAGCCTCACTCTCACAGG	58
5	5'-GGCTCTCTGTTGACTGTAGGGTTG 5'-TCTGTTTCTCAGATTACAAAGCCAA	58
6	5'-CGTAGGGATTCCCTCGTCTCATCT 5'-TTCAGGCTACTCTCTGCAACAGG	58
7	5'-GCATCGTGCTGCTGATTTC 5'-GAGCCCTTCTGGGAGAGGAG	58
8	5'-CGTGACCCAGAGAGACCTTACCT 5'-ACACCAGAGGAAGGATGTGTGAA	58
9	5'-GGGTACAGGAAGAGGCTTTGTTT 5'-CAACCTGTTCTGAAAGACATCGG	58
10	5'-CTCTCTCCCTCCTGTGTCCTG 5'-GGCTTCACACCAAGAAGTGTCTTA	58
11	5'-CGCACCTGTGGCAGTAACTA 5'-AGGCCTCGATGCTGTTTG	56
12	5'-TCCTCCTCTTAAGCCCTGATAGC 5'-TCAATACCTGCCTGGGTATTTCT	58
13	5'-CTGGTCTCGAACTCCTGTCCTCAG 5'-AGGCTTTCCTCTCACATGACCTACA	63
14	5'-GCATCCTGCCTACTGACCTG 5'-GAAAAGCGCTCTGAAACCTC	59
15	5'-TGCTGAGGATGCCTCTGTCT 5'-GCGACCCTTGTGTGGTAGA	59
16	5'-GTGTTCCCAGTCTGCCATTTT 5'-TGTGTGGACACTGTGTGACG	59
17	5'-CCTGGGGACTCACACTG 5'-CCTCACTTCCCGGACCAC	59

SPG7 RefSeq NM_003119.2

1
2
3 *Bioinformatics analysis.*
4

5 To build a three dimensional model of the C-terminal region of AFG3L2, the sequence
6
7 corresponding to residues 306-762 was submitted to PDB-blast
8
9 (<http://protein.cribi.unipd.it/pdbblast/>) that recognized the cell division bacterial protein FtsH with
10
11 an R-score of 1E-117. Its crystal structure was present in the protein database (PDB) as 2CE7,
12
13 which contains the AAA domain and a protease domain. Crystallization experiments of 2CE7 gave
14
15 rise to a tetragonal crystal form containing six monomers per asymmetric unit. These belong to two
16
17 virtually identical half-hexamers; the complete hexameric molecules are generated by a
18
19 crystallographic two-fold axis.
20
21

22
23 The AAA ring does not form a regular hexagon and the contacts of one AAA domain with the two
24
25 other interacting domains in the ring are much more asymmetric than those observed in the protease
26
27 domain.
28
29

30
31 As a result, three different monomer conformations are present in 2CE7 structure.
32

33
34 In order to build the AFG3L2 hexamer model, we constructed, three different models based on the
35
36 conformations of the three monomers present in 2CE7 structure, using the program NEST
37
38 (<http://trantor.bioc.columbia.edu/programs/jackal/index.html>). Subsequently to obtain the hexamer
39
40 model we superimposed them to the corresponding 2CE7 monomers in its hexamer using the
41
42 program SHEBA (Jung and Lee, 2000). Upon superimposition, the ADP molecule and the Mg²⁺
43
44 and Zn²⁺ ions were added to the model.
45
46

47
48 Using the program Yasara (www.yasara.org), we introduced the Thr654Ile, Met666Thr,
49
50 Met666Arg, Met666Val, Gly671Glu and Gly671Arg mutations. Next we refined the model using
51
52 the program Yasara with the protocol described below.
53

54
55 Each model was refined performing a 150 ps simulation of the homology models using the protocol
56
57 described in (Krieger, et al., 2004). It saves one PDB file every 25 picoseconds, and allows the user
58
59 to identify the best snapshot giving as output a table with force field energies, PhiPsi, Backbone and
60
Packing3 WHATIF checks (Vriend, 1990).

1
2
3 In order to choose the best conformer saved during the refinement procedure we derived a quality
4
5 parameter defined as follows:
6

$$7 \quad Q = (\text{Energy}/10000) - (\text{PhiPsi} + \text{Backbone} + \text{Packing3}) = \text{quality}$$

8
9
10 The conformer having the lowest value of Q was selected for subsequent analyses.

11
12 Data on the electric dipole moment calculated using the Yasara software. The difference of
13
14 electrostatic potential (mV) was calculated from the measure of the electric dipole moment using

15
16 the formula: $\Delta V = \frac{d}{(4\pi \cdot r^2 \cdot \epsilon_0)}$. D = electric dipole moment; r = distance between examer surfaces;
17
18

19
20 ϵ_0 = electric constant in vacuum.
21

22
23 The pH of the AFG3L2 hexamer catalytic site was calculated using pH Calculator software
24
25 (<http://www.webqc.org/phsolver.php>). pKa values were obtained from the PROPKA software ver
26
27 2.0 (Guerois, et al., 2002). We calculated the pH of normal hexamer and hexamers containing
28
29 identified mutations for all aminoacids distant <0.5 nm from the Zn atom within the catalytic site
30
31 (constant arbitrary concentration set at 0.01M).
32

33
34 The energetic stability of AFG3L2 protein and the interaction energy of each monomer were
35
36 calculated using the FoldX software ver 3.0 (Guerois, et al., 2002). We calculated both the
37
38 interaction energy between one monomer and the two flanking monomers, and between one
39
40 monomer and the remaining hexamer.
41
42

43
44 To verify the possible three-dimensional structure of AFG3L2 homopolymer or heteropolymer, a
45
46 3D model of the C-terminal tract of SPG7, a known interactor of AFG3L2 (Atorino, et al., 2003)
47
48 was also created following the same protocol as above.
49

50
51 Homo- and Heteropolymers were reconstructed with the software NEST and SHEBA (Jung and
52
53 Lee, 2000; Petrey, et al., 2003).
54

55
56 Finally, the software PoPMuSic estimated the stabilizing/destabilizing effect of each aminoacidic
57
58 substitution, through the measurement of the free energy difference ($\Delta\Delta G$) of the molecule (Gilis
59
60 and Rooman, 2000).

Supp. Table S3. *AFG3L2* variants found in 366 ADCA patients.

Variants	Exon / Intron	Patients	Controls	Notes
rs12327346:C>G	EX1	20/366	7/95	
c.-92T>C		1/366	0/95	
c.-71C>T		4/366	1/95	
c.-48G>A		2/366	0/95	
c.-32C>T		1/366	0/95	
c.293-33G>A	IVS3	1/366	0/95	The variant does not alter splicing
c.293-13_293-14delTT		2/366	0/95	The variant does not alter splicing ¹
c.400-14C>G	IVS4	4/366 ²	0/95	The variant does not alter splicing
c.718C>A (p.=)	EX7	1/366	n.a.	The variant does not alter splicing
rs8097342:G>A	IVS7	120/366	n.a.	
rs8091858:C>T	IVS8	27/366	0/95	
c.1027-12T>C		2/366	0/95 ³	The variant does not alter splicing
rs9966470:A>T	IVS9	85/366	21/95	
c.1165-24G>A		5/366	1/95	
c.1319-59G>T	IVS10	3/366	0/95	The variants does not alter splicing
c.1319-40C>T		1/366	0/95	The variants does not alter splicing
rs11080572:G>A	EX11	349/366 ⁴	85/95 ⁵	
c.1426+21_1426+22insCAGGTC	IVS11	1/366	0/95	The variant does not alter splicing
c.1479G>A (p.=)	EX12	1/366	0/95	The variant does not alter splicing
rs11553521:A>G	EX13	125/366	26/95	
c.1664-39G>A	IVS13	8/366	2/95	
c.1664-9T>C		1/366	0/95	The variant does not alter splicing
c.2175+18G>A	IVS16	9/366	4/190 ⁶	
rs1129115:G>C	EX17	117/366	26/95	
c.2325C>T (p.=)		1/293	0/95	Not found in an affected niece

In bold, variants not found among controls and/or in the dbSNP(129). Controls were all of French origin, except for note 3 - 95 Italian controls, and note 6 - 95 Italian and 95 French controls; 1-The effect on splicing was tested using a minigene assay (see Supp. Materials and Methods); 2-The c.400-14C>G variant was tested in one family and did not segregate from the affected father to the affected son; 4-Two hundred-24 cases were homozygous (A/A) and 125 heterozygous (G/A); n.a. = not available; 5-Fifty-seven controls were homozygous (A/A) and 28 heterozygous (G/A).

Supp. Table S4. Mutation effect on the electric dipole of the translocation channel and on the potential difference between the inner mitochondrial membrane side and the matrix side of the hexamer.

	<i>Potential difference - PD (mV)</i>	<i>PD compared to wild type (mV)</i>	<i>PD compared to wild type (%)</i>	<i>Electric dipole (C m)</i>
wt	22,274			$1,79 \times 10^{-26}$
T654I	22,60	0,33	1,48%	$1,82 \times 10^{-26}$
M666V	22,305	0,031	0,14%	$1,79 \times 10^{-26}$
M666T	22,945	0,671	3,01%	$1,85 \times 10^{-26}$
M666R	19,548	-2,726	-12,24%	$1,57 \times 10^{-26}$
G671E	25,736	3,462	15,54%	$2,07 \times 10^{-26}$
G671R	18,887	-3,387	-15,21%	$1,52 \times 10^{-26}$

Yellow = wild-type (wt) values; Green = lower dipole and potential difference; Blue = dipole and potential difference not significantly different from the wild-type; Red = higher dipole and potential difference. mV = millivolts; C m = Coulomb meter.

Supp. Table S5. Mean interaction energy [§] (Kcal/Mol) between each monomer of the AAA-protease (A to F) and the other five monomers

	Monomer						Mean ¹
	A	B	C	D	E	F	
wt	-49.89	-79.31	-57.50	-59.64	-82.24	-54.58	-63.86
T654I	-43.23	-76.66	-66.77	-55.32	-76.86	-57.56	-62.73
M666V	-56.73	-83.46	-51.03	-37.19	-60.82	-56.99	-57.70
M666T	-50.50	-64.60	-46.42	-48.36	-76.81	-58.26	-57.49
M666R	-35.73	-71.15	-49.36	-37.83	-58.24	-42.46	-49.13
G671E	-49.41	-79.02	-54.77	-61.61	-77.72	-50.24	-62.13
G671R	-51.46	-70.63	-59.66	-38.88	-64.79	-50.73	-56.03

¹Yellow = wild-type (wt) interaction; Green = lower interaction; Blue = slightly lower interaction

[§] Interaction energy was calculated using the application FoldX ver3.0 (Guerois R et al., 2002)